Materials Chemistry and Physics 224 (2019) 40–46

Contents lists available at ScienceDirect

Materials Chemistry and Physics

journal homepage: www.elsevier.com/locate/matchemphys

Synthesis and characterization of a novel fluorosilicone resin based on trifluoropropylalkoxylsilane

Yuetao Liu, Dan Zhu, Jiawen Sun, Jie Li, Yumin Wu, Chuanhui Gao*

College of Chemical Engineering, Qingdao University of Science & Technology, Qingdao, 266042, China

HIGHLIGHTS

- A novel fluorosilicone resin (FSR) was synthesized based on trifluoropropylalkoxylsilane.
- FSR had random molecular structures and lower T_g.
- The cured FSR possessed high thermal stability and good mechanical properties.
- The cured FSR had hydrophobic surface.

GRAPHICAL ABSTRACT

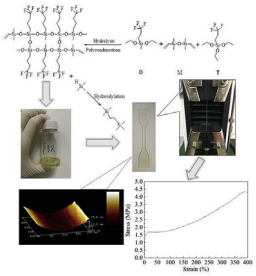

ARTICLE INFO

Keywords:
Fluorosilicone resin
Hydrolysis-polycondensation
Trifluoropropylalkoxylsilane
Synthesis
Properties

ABSTRACT

A novel type of fluorosilicone resin (FSR) based on trifluoropropylalkoxylsilane (T monomer) was synthesized using hydrolysis-polycondensation method and cured by hydrosilylation reaction. The molecular structure of FSR was characterized by FTIR and NMR spectra. The property of the cured FSR was also investigated. TGA/DTG showed the good thermal stability of the cured FSR because of no residual terminal hydroxyl groups in FSR molecular structure. The higher molar ratios of trifluoropropyl ($-CH_2CH_2CF_3$) and methyl groups (F/R molar ratios) lowered the thermal stability. DSC results indicated the only one T_g of each cured FSR and it varied from $-52.0\,^{\circ}C$ to $-13.2\,^{\circ}C$. Furthermore, the cured FSR possessed good mechanical properties that the tensile strength could exceed 2.0 MPa and the elongation at break was higher than 300%. The increase of F/R molar ratios lowered the surface free energy of the cured FSR from 24.20 mN/m to 22.98 mN/m which indicated the surface hydrophobicity improved. The water and n-hexadecane contact angles were 110.4° and 34.2° that might be attributed to the smooth surfaces characterized by SEM and AFM.

1. Introduction

Recently, significant attention had been drawn to prepare low surface energy materials used as hydrophobicity and self-cleaning coatings. So there existed a demand to construct hydrophobic materials which were easy to prepare on large scale. Fluorosilicone resin (FSR), characterized by the high cross-linked Si-O-Si backbone with trifluoropropyl pendant groups ($-CH_2CH_2CF_3$), was an obvious choice for hydrophobic applications due to their merits, such as high thermal stability, low temperature flexibility, radiation resistance, low surface energy and outstanding fuel and chemical resistance because of the introducing of fluorine atoms into the polymer structure [1–3].

As we known, silicone resin appeared earlier than silicone oil or elastomer. And there were four possible functional units existed in molecular structure which were conveniently designated by letters as follows: M for monofunctional $R_3SiO_{1/2}$ units, D for difunctional

* Corresponding author.
E-mail address: gaochuanhui@qust.edu.cn (C. Gao).

https://doi.org/10.1016/j.matchemphys.2018.11.077

Available online 03 December 2018

$R_2SiO_{2/2}$ units, T for trifunctional $RSiO_{3/2}$, and Q for tetrafunctional $SiO_{4/2}$ units. The most common molecular structure included D and T units (D/T resin) or M and Q units (M/Q resin). They were generally synthesized by hydrolysis-polycondensation method with acid or alkaline compounds as catalysts using T or D monomers, such as chlorosilane or alkoxysilane [4]. And lots of work had been done. For example, the synthesis of M/Q, D/Q or M/D/T type methylsilicone resin (MSR) [1,5,6] or phenylsilicone resin (PSR) [7], the functionalization by phenyl [8], silphenyl [2,9,10] or cycloaliphatic epoxy [11] and the reinforcement by polyhedral oligomeric silsesquioxanes [12], glass fabric [13], carbon fiber [14,15], graphene [16], etc.

However, little works were focused on FSR until now. Lots of work were focused on the low or high molecular weight linear polyfluorosiloxane which was synthesized by cationic or anionic open-ringing polymerization of D monomers, such as 1,3,5-tris(3,3,3-trifluoropropyl)methylcyclotrisiloxane (D_3F) [17–19]. Why? The reason might be the high hydrolytic activity or corrosive nature of the T monomer for FSR synthesis, especially trifluoropropyltrichlorosilane [20,21]. The high hydrolytic activity should be responsible for the self-condensation to form gel particles and the corrosive nature could bring about significant risks of handling and disposal. Over the past few years, trifluoropropyalkoxylsilane was widely used to synthesis fluorinated polyhedral oligomeric silsesquioxane (F-POSS) as ultra-hydrophobic materials [22–24]. Here, trifluoropropyalkoxylsilane as T monomer for FSR synthesis using hydrolysis-polycondensation method was put forward to overcome the above shortcomings.

In this paper, a novel FSR was synthesized using a hydrolysis-polycondensation method with trifluoropropylmethyldiethoxylsilane as D monomer and trifluoropropyltriethoxylsilanes as T monomer to minimize the hydrolytic activity difference of each reactant. At the same time, the vinyl groups were incorporated with 1,3-divinyltetramethylsiloxane as M monomer. The obtained FSR was cured with hydrogen-containing fluorosilicone oil (FSR-H) by hydrosilylation reaction [25,26]. The molecular structure of FSR was characterized by FTIR, ^{1}H NMR and ^{29}Si NMR spectra. The properties of cured FSR were investigated by TGA/DTG, DSC, the stress-strain tests, hardness, SEM, AFM and the contact angle. The effects of molar ratios of trifluoropropyl and methyl groups (F/R molar ratios) on the properties of cured FSR were also studied.

2. Experimental

2.1. Materials

Trifluoropropylmethyldiethoxylsilane (D monomer) and trifluoropropyltriethoxylsilanes (T monomer) were purchased from Zhejiang Feidian Chemical Co., Ltd. 1,3-divinyltetramethylsiloxane (M monomer) was obtained from Shandong Wanda Organosilicon New Materials Co., Ltd. FSR-H was synthesized with D_3F as monomer and 1,3-dihydrogentetramethylsiloxane as end capping agent by cationic open-ringing polymerization. The hydrogen content was calculated based on the peak area at about 4.8 ppm of ^{1}H NMR. All other chemicals were used as received unless otherwise mentioned.

2.2. Synthesis and curing

A series of FSR was synthesized by a hydrolysis-polycondensation method using M, D and T monomers with acid as catalyst for hydrolysis and base as catalyst for polycondensation. For example, acidic water (12.6 g, 0.7 mol) which consisted of hydrochloric acid (3.5 g) and trifluoromethanesulfonic acid (0.5 g) was added to a four-neck flask. A solution of M (4.65 g, 0.025 mol), D (11.5 g, 0.05 mol), T (51.2 g, 0.2 mol) and ethyl acetate (100 ml) was added drop-wise to the flask at room temperature. After completed, the solution was heated to 80 °C and stirred for 6 h to further hydrolysis. Then the obtained solution was separated in a separating funnel. The organic phase was washed with distilled water until pH = 7 and dried with anhydrous calcium chloride for 12 h. The product was added to a four-neck flask and heated to 120 °C for 4 h with potassium hydroxide as catalyst to further polycondensation. The colorless transparent liquid was obtained after the remove of low-boiling residues through reduced pressure distillation at 150 °C for 2 h. All the synthesized FSR informations were listed in Table 1. FSR was cured with FSR-H by hydrosilylation reaction according to the found -Si–H and -Si–CH=CH_2 molar ratios with Karstedt's catalyst [27]. The curing was conducted at 80 °C for 1 h to obtain transparent films.

Table 1
Information of the synthesized FSR.

No.	M/D/T[b]	F/R[c]		Viscosity (mPa·S)	Yield (%)
		Designed	Found[a]		
FSR-1	1/1/1	0.33	0.37	2350	83.4
FSR-2	1/1/2	0.43	0.46	2700	82.6
FSR-3	1/1/3	0.50	0.52	3150	84.1
FSR-4	1/1/4	0.56	0.54	4300	82.0
FSR-5	1/1/5	0.60	0.58	5200	81.5

[a] Calculated by ^{1}H NMR.
[b] The molar ratio of M, D and T units.
[c] The molar ratio of trifluoropropyl groups to methyl groups.

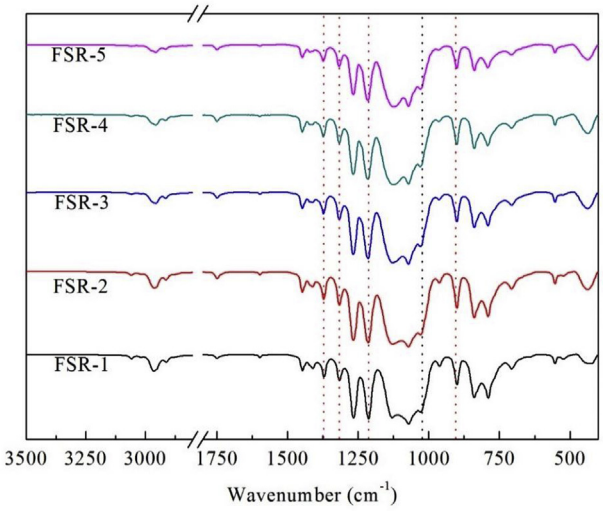

Fig. 1. FTIR spectra of FSR.

2.3. Characterization

FTIR spectra were measured using the standard KBr-pellet technique on a Bruker TENSOR27 infrared spectrophotometer. Each spectrum was recorded by performing 32 scans between 4000 and 400 cm^{-1}. ^{1}H NMR and ^{29}Si NMR spectra were conducted on a Bruker AV400 NMR spectrometer at 400 MHz (^{1}H) and 79 MHz (^{29}Si) in $CDCl_3$, respectively. Chemical shifts (δ) were expressed in ppm downfield from tetramethylsilane (TMS) as an internal standard. TGA/DTG were carried out on a SDTQ600 thermo-analyzer from room temperature to 700 °C at a heating rate of 10 °C/min under nitrogen atmosphere (50 mL/min). DSC was performed on a Rheometric Scientific DSC SP at a heating rate of 10 °C/min from −150 °C to room temperature under nitrogen atmosphere (25 mL/min). The stress-strain tests were performed on an Instron model 4411 tester, controlled by Series IX software. Dog-bone shaped specimens (ASTM D1708) were cut and tests were conducted at room temperature using a 25.0 mm/min cross-head speed. For each cured FSR at least three samples were tested and the average values of hardness, ultimate tensile strength and elongation at break values were

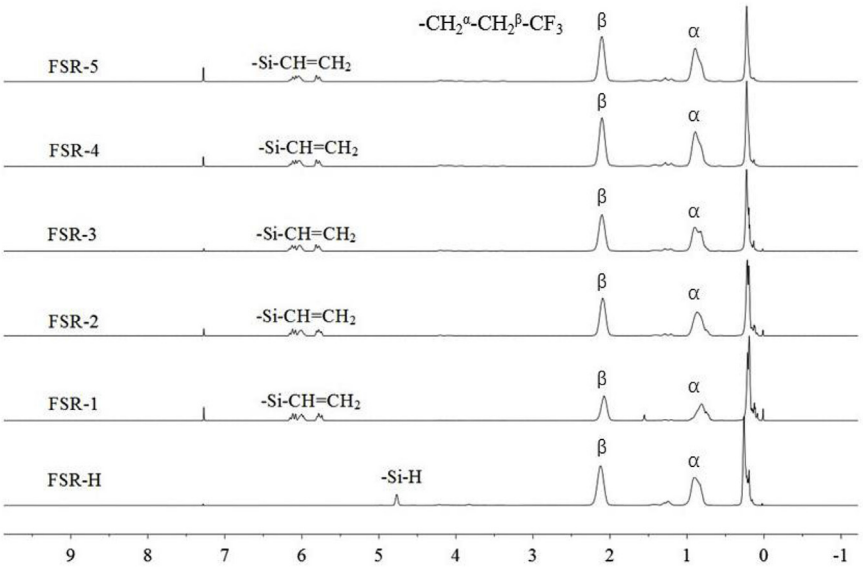

Fig. 2. ^{1}H NMR of FSR

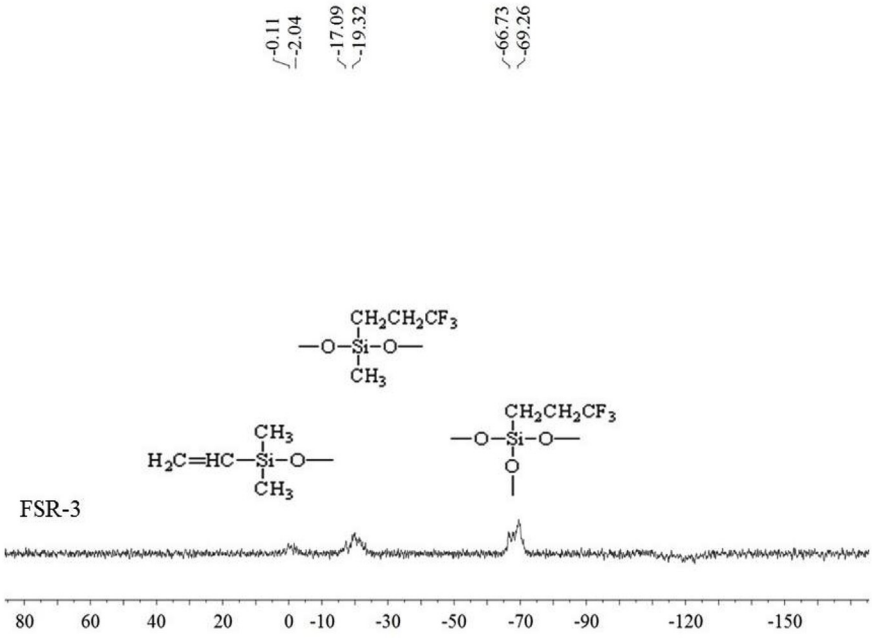

Fig. 3. ^{29}Si NMR of FSR

obtained. Testing of hardness was carried out using a Shore type A Durometer in accordance with ASTM D2240. The surface morphology of cured FSR was observed by scanning electron microscope (JSM-7600F, JEOL) and atomic force microscope (MULTIMODE8). Contact angles of cured FSR were measured by the sessile drop method at room temperature using a Rame-hart NRL contact angle goniometer (model 100, Landing, NJ). Five droplets were placed at various spots on the substrate surface and the average readings were reported. Wetting liquids used for contact measurements were water and n-hexadecath. Surface free energy was calculated from the measured contact angles according to the extended Fowkes equation [28].

$$\gamma_i = \gamma_i^d + \gamma_i^p \tag{1}$$

$$\gamma_i \times (1 + \cos\theta) = 2 \times [(\gamma_i^d \gamma_s^d)^{1/2} + (\gamma_i^p \gamma_s^p)^{1/2}] \tag{2}$$

where γ_i was the surface tension of wetting liquid, γ_i^d and γ_i^p were the dispersive and polar forces components, respectively. γ_s^d and γ_s^p could be calculated by substituting values for water ($\gamma_i^d = 21.8mN/m$; $\gamma_i^p = 51.0mN/m$) and n-hexadecath ($\gamma_i^d = 27.5mN/m$; $\gamma_i^p = 0mN/m$) into Eq. (2) and solving the corresponding set of simultaneous equations. The total surface energy γ was the summation of γ_s^d and γ_s^p.

3. Results and discussion

3.1. FTIR

Fig. 1 showed the FTIR spectra of FSR with different F/R molar ratios. The peak at 1030 cm^{-1} was selected as an internal reference to eliminate the dosage effect of FSR samples. Obviously, the broad and strong absorption peaks from 1070 cm^{-1} to 1130 cm^{-1} attributed to the Si-O-Si asymmetric stretching vibration were observed. This illustrated the formation of FSR molecular structure through the hydrolysis-polycondensation of M, D and T monomers. The peaks at about 1270 cm^{-1} ascribed to the absorption of -Si-CH$_3$ structural vibration,

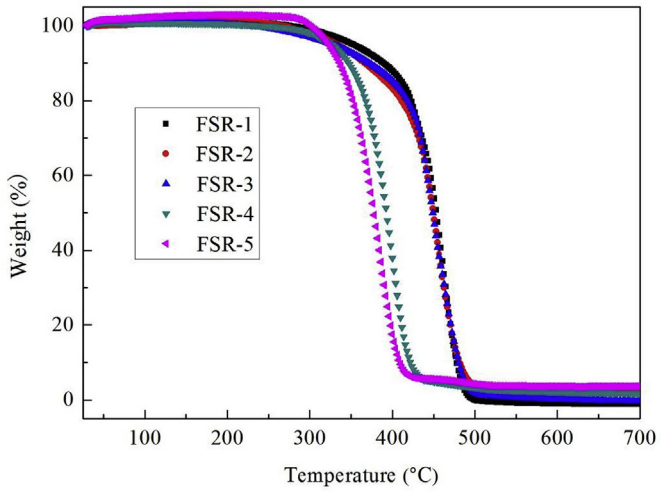

Fig. 4. TGA curves of cured FSR.

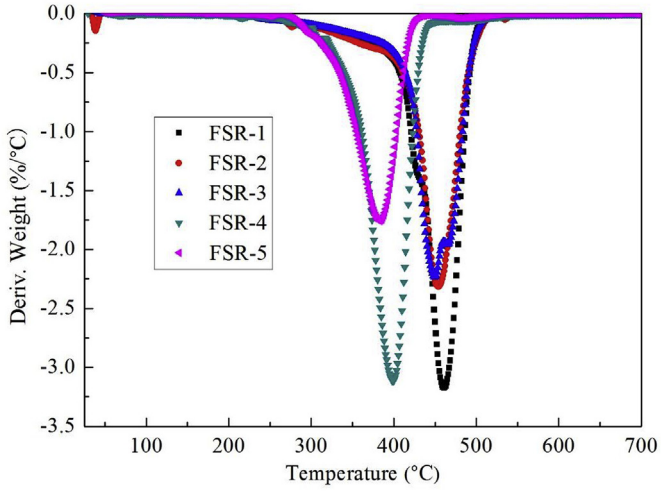

Fig. 5. DTG curves of cured FSR.

gradually shifted from 1270 cm^{-1} to 1276 cm^{-1} with the increase of F/R molar ratios. It could be explained by the stronger polarity of $-CH_2CH_2CF_3$ units [18]. The characteristic absorption peaks of $-CH_2CH_2CF_3$ units appeared at 1376 cm^{-1} (wagging $-CH_2-$), 1320 cm^{-1} ($-CH_2-CH_2-$), 1220 cm^{-1} ($-CF_3$) and 902 cm^{-1} ($-C-CF_3$), were marked with the red dotted lines. And the absorption intensities increased with the increase of F/R molar ratios. The weak peaks at 1602 cm^{-1} and 3056 cm^{-1} corresponded to Si-CH = CH_2 were also noticed in spectra. The FTIR results verified the incorporation of M, D and T monomers to FSR molecular structure. Moreover, there was no evidence of any residual terminal hydroxyl groups because the characteristic peaks of -Si-OH from 3200 cm^{-1} to 3390 cm^{-1} were not observed. So FSR possessed high thermal resistance and it was further discussed below.

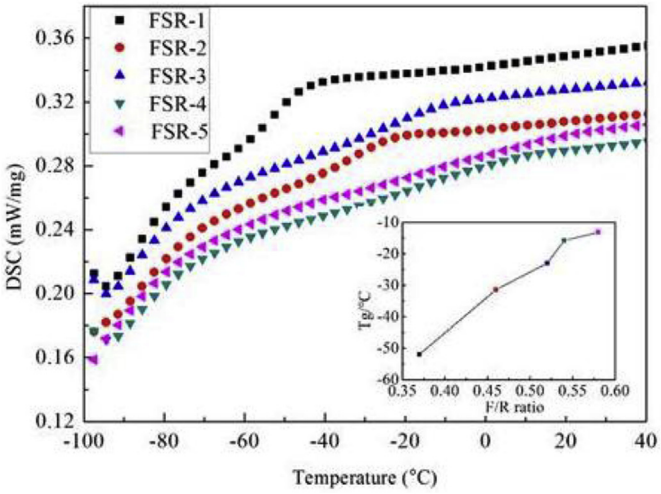

Fig. 6. DSC curve of cured FSR.

3.2. NMR

Whether the found and the designed F/R molar ratios were equal, it would be discussed in ^1H NMR and ^{29} Si NMR analyses, which were shown in Fig. 2 and Fig. 3, respectively. The chemical shift about 0.2 ppm was produced by -Si–CH_3 and the peaks at 0.87 ppm and 2.10 ppm were corresponded to the α-hydrogen and β-hydrogen in $-CH_2^{\alpha}-CH_2^{\beta}-CF_3$ units. The triplet appeared between 5.7 and 6.1 ppm was produced by Si–CH = CH_2. Because the added amount of M units was so little that the peaks exhibited in spectra were very weak which was corresponding to the FTIR results. The quantitative analysis of the ^1H NMR spectra was performed via integrating the peaks in each spectra. The values of F/R molar ratios were calculated based on the peak area of signals at 0.87 ppm and 0.2 ppm. The results were presented in Table 1. Because of the loss of monomers during the synthesized process and the generation of the low-boiling siloxane residues, the found F/R molar ratios were not equal to the feeding amount. Also the peak at about 4.7 ppm was observed which was produced by Si-H from the synthesized FSR-H. The calculated hydrogen molar content was 16.7%.

As the same trend of ^{29} Si NMR, the spectra of FSR-3 was chosen as the example to discuss and shown in Fig. 3. The characteristic peaks at about 69.26 ppm were ascribe to the 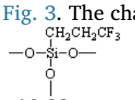 units. The chemical shifts at about 19.32 ppm and 2.04 ppm were produced by 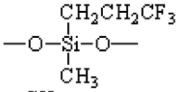 and 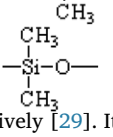 units, respectively [29]. It further confirmed the molecular structure of the synthesized FSR.

Table 2
TGA data of cured FSR obtained under N_2 atmosphere.

No.	Onset degradation temperature/°C	Temperature for 5% mass loss/°C	Temperature for 10% mass loss/°C	Temperature for maximum degradation rate/°C
FSR-1	310	353	389	460
FSR-2	303	340	372	454
FSR-3	301	334	368	449
FSR-4	305	327	347	399
FSR-5	305	323	336	362

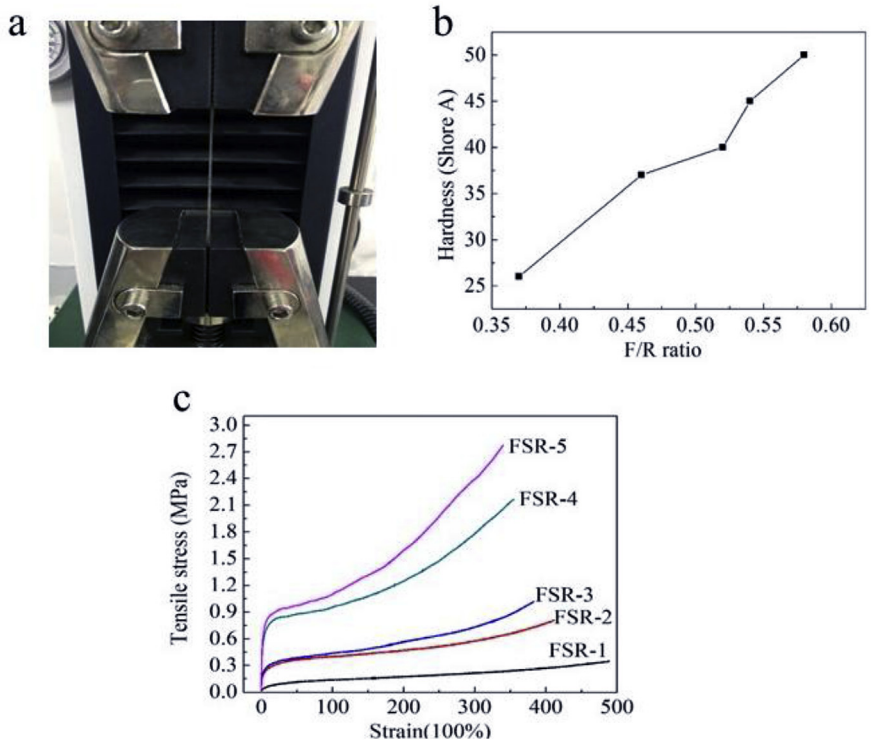

Fig. 7. Mechanical properties of cured FSR. a, Photographs of a cured FSR film during stretching process. b, Hardness of cured FSR with different F/R ratios. c, Stress-strain curves of cured FSR.

Table 3
Contact angles data of cured FSR.

Sample no.	Contact angle (°)		Surface free energy (mN/m)		
	Water	n-hexadecath	γ_s^d	γ_s^p	γ_l
FSR-1	96.1	37.9	22.00	3.07	24.20
FSR-2	98.6	37.4	22.13	2.60	23.80
FSR-3	100.3	36.4	22.38	2.36	23.58
FSR-4	104.3	35.0	23.93	1.58	23.27
FSR-5	110.4	34.2	24.94	1.19	22.98

3.3. TGA/DTG

Fig. 4 and Fig. 5 showed the TGA/DTG curves of cured FSR in nitrogen atmosphere. The characteristic data were listed in Table 2. It could be observed that the thermal stability of cured FSR was declined with the increase of F/R molar ratios. All the onset degradation temperatures, the temperatures for 5% mass loss, the temperatures for 10% mass loss and the temperatures for maximum degradation rate gradually decreased with the increase of -$CH_2CH_2CF_3$ units. It's also observed that the degradation of all the five samples just experienced one stage which meant the samples just undergone one degradation mechanism with the temperature elevated. As previously reported, degradation of silicone resins was caused by dehydration and "unzipping degradation" resulted from residual terminal hydroxyl groups [9]. The FTIR results already proved there existed no hydroxyl groups in FSR molecular structure, so the cured FSR possessed good temperature stability. For example, the onset degradation temperatures and the temperatures for maximum degradation rate of all the cured FSR were higher than 300 °C and 360 °C, respectively. It's clear that the increasing of the F/R molar ratios which meant the increasing of -$CH_2CH_2CF_3$ units lowered the thermal temperature stability. This was because not only the end depolymerization and random degradation occurred, but also the side chains of FSR start to rupture and trifluoropropene was generated [30]. Furthermore, the cured FSR nearly completely decomposed in nitrogen atmosphere and there were no residues left.

3.4. DSC

DSC was performed to investigate the crystalline behavior and the glass transition temperature (T_g) of cured FSR. The results were presented in Fig. 6. There was only one T_g in each curves and T_g gradually increased from −52.0 °C to −13.2 °C as the F/R molar ratios increased. It was also noticed that no melting peaks existed in the curves. In other words, there were no crystalline regions in cured FSR. This could be attributed to the fact that the introduction of the -$CH_2CH_2CF_3$ units increased the rigidity of the molecular chain and broke the symmetry and regularity, making cured FSR hard to crystallize.

3.5. Mechanical properties

The mechanical properties of cured FSR performed via the stress-strain tests and the stretching process were shown in Fig. 7. The hardness was also measured and included in Fig. 7. As expected, the hardness and the tensile strength increased from 26 to 50 Shore A and from 0.35 MPa to 2.78 MPa with the increasing of the F/R molar ratios, respectively. Conversely, the elongation at break decreased from 458.4% to 331.7%. This was because the T monomer increased with the increase of F/R molar ratios which meant the high cross-linked density. That was to say, the mechanical properties of cured FSR could be altered though F/R molar ratios according to the application performance.

3.6. Contact angle measurement

The hydrophobicity of cured FSR was investigated based on the contact angle measurements and surface free energy calculations. The values of measured and calculated parameters with different F/R mass ratios were listed in Table 3. The water contact angles of cured FSR

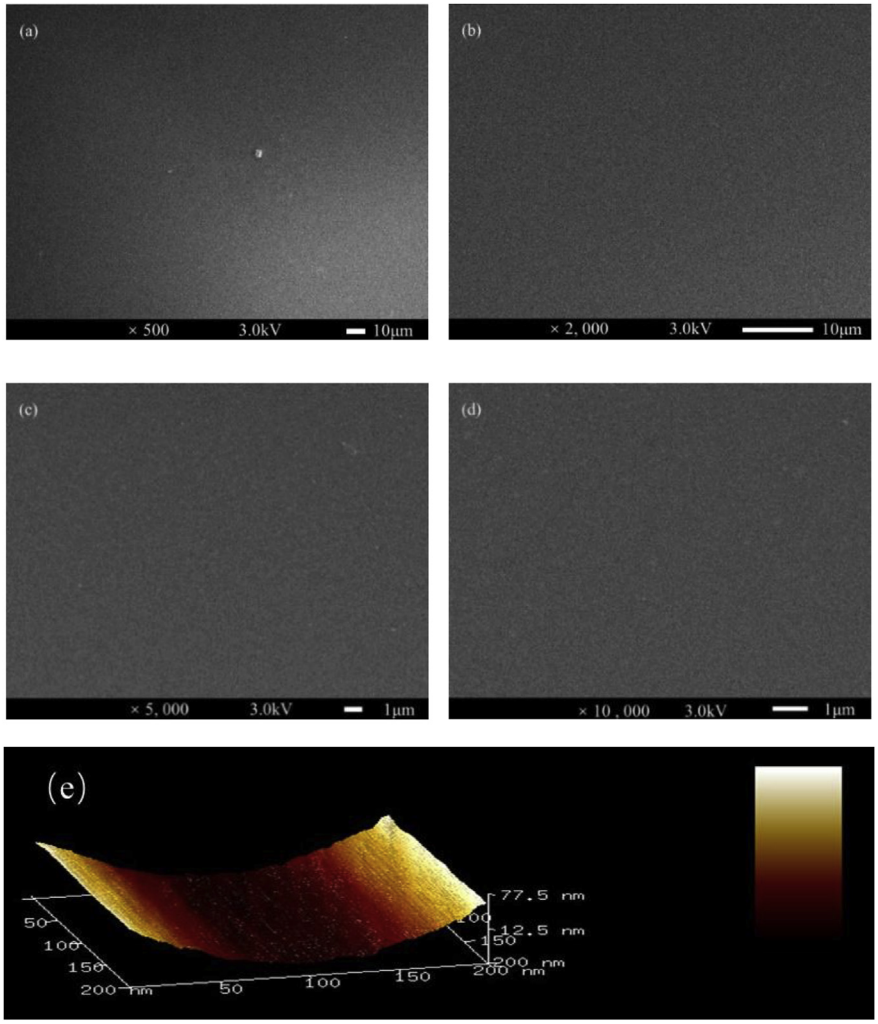

Fig. 8. The surface morphology of cured FSR-3. a, b, c and d, SEM images of FSR-3 at 500, 2000, 5000 and 10000 times. e, AFM micrographs of FSR-3 presented as 3D-views of height data.

increased from 96.1° to 110.4° with the increase of the F/R molar ratios. Conversely, the n-hexadecane contact angles varied from 37.9° to 34.2°. It indicated that the cured FSR possessed hydrophobic surface. With-$CH_2CH_2CF_3$ units increased, the hydrophobicity improved. Besides, the surface free energy decreased from 24.20 mN/m to 22.98 mN/m. This further explained the hydrophobicity of cured FSR. However, the hydrophobicity might not be as satisfactory as we thought. It's reported that the cross-linked silcones had a contact angle of 109° [31]. And why? It's well known that hydrophobicity was a function of both surface free energy and surface roughness [32]. The surfaces morphology of cured FSR were examined by SEM and AFM. The results were shown in Fig. 8 and FSR-3 was chosen as example to illustrate. It could be observed that no matter how many magnification times, 500, 2000, 5000 or 10000, the surface of cured FSR-3 was smooth. AFM micrographs of FSR-3 presented as 3D-views of height data in Fig. 8(e) also proved the conclusion. This might explain the unsatisfactory hydrophobicity of cured FSR. And it would be further focused in the following study.

4. Conclusion

In summary, a novel FSR was synthesized by M, D and T monomers though a hydrolysis-polycondensation method and cured by hydrosilylation reaction. TGA/DTG results indicated cured FSR possessed good thermal stability because of no residual terminal hydroxyl groups existed in FSR according to the FTIR and NMR spectra. However, the increasing of F/R molar ratios damaged the high temperature stability. The cured FSR undergone one degradation mechanism and nearly completely decomposed in nitrogen atmosphere. DSC results showed that the cured FSR had one T_g and it varied from −52.0 °C to −13.2 °C with the increase of F/R molar ratios. The cured FSR possessed good mechanical properties and it could be altered though F/R molar ratios according to the application performance. For example, the tensile strength could vary from 0.35 MPa to 2.78 MPa and the elongation at break could increase from 330% to 450%, respectively. The water contact angles of cured FSR increased with the increase of F/R molar ratios. By contrast, the n-hexadecane contact angles and surface free energy lowered which indicated the hydrophobicity improved. However, the hydrophobicity properties might not be as satisfactory as we thought. The smooth surfaces examined by SEM and AFM might explain this phenomenon. The cured FSR could be used as promising alternative materials for hydrophobic applications in the future.

Acknowledgments

This work was supported by Research Award Fund for Outstanding Young and Middle-aged Scientists of Shandong Province (Grant No. BS2015CL019); Major science and technology innovation project of Shandong province (Grant No. 2017CXGC1104); Shandong Provincial Natural Science Foundation (Grant No. ZR2018MB034).

References

[1] L. Bourget, P.H. Mutin, A. Vioux, J.M. Frances, J. Polym. Sci., Part A: Polym. Chem. 36 (1998) 2415–2425.
[2] M. Jia, C. Wu, W. Li, D. Gao, J. Appl. Polym. Sci. 114 (2009) 971–977.
[3] X. Yang, Q. Shao, L. Yang, X. Zhu, X. Hua, Q. Zheng, G. Song, G. Lai, J. Appl. Polym. Sci. 127 (2013) 1717–1724.
[4] D.W. Mosley, G. Khanarian, D.M. Conner, D.L. Thorsen, T. Zhang, M. Wills, J. Appl. Polym. Sci. 131 (2014) 1082–1090.
[5] F. Sun, Y. Hu, H.G. Du, J. Appl. Polym. Sci. 125 (2012) 3532–3536.
[6] Q. Mu, D. Peng, W. Ju, F. Zhang, C. Wang, J. Appl. Polym. Sci. 132 (2015).
[7] J. Chen, Z. Fu, H. Huang, X. Zeng, Z. Chen, RSC Adv. 6 (2016).
[8] M. Smith, J. Appl. Polym. Sci. 128 (2013) 4189–4200.
[9] Z. Yang, S. Han, R. Zhang, S. Feng, C. Zhang, S. Zhang, Polym. Degrad. Stab. 96 (2011) 2145–2151.
[10] Z. Yang, L. Feng, D. Shen, S. Feng, C. Zhang, Thermochim. Acta 521 (2011) 170–175.
[11] N. Gao, W.Q. Liu, Z.L. Yan, Z.F. Wang, Opt. Mater. 35 (2013) 567–575.
[12] Y. Zhang, Y.W. Li, J. Zheng, H.L. Guo, X.X. Guan, M.G. Lu, K. Wu, L.Y. Liang, J. Appl. Polym. Sci. (2015) 132.
[13] B. Zhu, Y. Wu, H.H. Reese, D.E. Katsoulis, F.J. Mcgarry, Macromol. Mater. Eng. 291 (2006) 1052–1060.
[14] Y.C. Qing, W.C. Zhou, S. Jia, F. Luo, D.M. Zhu, Appl. Phys. A 100 (2010) 1177–1181.
[15] G. Wu, L. Ma, Y. Wang, L. Liu, Y. Huang, RSC Adv. 6 (2016) 5032–5039.
[16] D. Gui, S. Yu, W. Xiong, X. Cai, C. Liu, J. Liu, RSC Adv. 6 (2016) 35210–35215.
[17] H.F. Fei, W. Xie, Q. Wang, X. Gao, T. Hu, Z. Zhang, Z. Xie, RSC Adv. 4 (2014) 56279–56287.
[18] B. Li, S. Chen, J. Zhang, Polym. Chem. 3 (2012) 2366–2376.
[19] M. Barrère, C. Maitre, a.M.A. Dourges, P. Hémery, Macromolecules 34 (2001) 7276–7280.
[20] M.J. M, V. Ashwani, I.S. T, V.B. D, Angew. Chem. Int. Ed. 47 (2010) 4137–4140.
[21] B. Wang, T. Qian, Q. Zhang, X. Zhan, F. Chen, Surf. Coat. Technol. 304 (2016) 31–39.
[22] X. Wang, Q. Ye, J. Song, C. Cho, C. He, J. Xu, RSC Adv. 5 (2015) 4547–4553.
[23] S.T. Iacono, A. Vij, W. Grabow, S.D. Jr, J.M. Mabry, Chem. Commun. 47 (2008) 4992–4994.
[24] J. He, K. Yue, Y. Liu, X. Yu, P. Ni, K.A. Cavicchi, R.P. Quirk, E.Q. Chen, S.Z.D. Cheng, W.B. Zhang, Polym. Chem. 3 (2012) 2112–2120.
[25] W.S. Lee, K.S. Yeo, A. Andriyana, Y.G. Shee, F.R.M. Adikan, Mater. Des. 96 (2016) 470–475.
[26] M. Wójcik-Bania, A. Krowiak, J. Strzezik, M. Hasik, Mater. Des. 96 (2016) 171–179.
[27] M. Dascalu, S.J. Dünki, J.E.Q. Quinsaat, Y.S. Ko, D.M. Opris, RSC Adv. 5 (2015) 65–71.
[28] F. Hansen, University of Oslo, (2004).
[29] E.A. Williams, Annu. Rep. NMR Spectrosc. 15 (1984) 235–289.
[30] H. Kählig, P. Zöllner, B.X. Mayer-Helm, Polym. Degrad. Stab. 94 (2009) 1254–1260.
[31] J.T. Han, D.H. Lee, C.Y. Ryu, K. Cho, J. Am. Chem. Soc. 126 (2004) 4796–4797.
[32] J.M. Mabry, S.T. Iacono, A. Vij, B.D. Viers, (2007).